

Published in final edited form as:

*Int J Mass Spectrom.* 2011 March 1; 300(2-3): 143–148. doi:10.1016/j.ijms.2010.06.027.

# Ion Behavior in an Electrically Compensated Ion Cyclotron Resonance Trap

Adam M. Brustkern, Don L. Rempel, and Michael L. Gross

Department of Chemistry, Washington University in St. Louis, One Brookings Drive, Box 1134, St. Louis, Missouri, USA

## **Abstract**

We recently described a new electrically compensated trap in FT ion cyclotron resonance mass spectrometry and developed a means of tuning traps of this general design. Here, we describe a continuation of that research by comparing the ion transient lifetimes and the resulting mass resolving powers and signal-to-noise (S/N) ratios that are achievable in the compensated vs. uncompensated modes of this trap. Transient lifetimes are ten times longer under the same conditions of pressure, providing improved mass resolving power and S/N ratios. The mass resolving power as a function of m/z is linear (log-log plot) and nearly equal to the theoretical maximum. Importantly, the ion cyclotron frequency as a function of ion number decreases linearly in accord with theory, unlike its behavior in the uncompensated mode. This linearity should lead to better control in mass calibration and increased mass accuracy than achievable in the uncompensated mode.

## 1. Introduction

Ion motion in the Penning trap used in Fourier transform ion cyclotron resonance mass spectrometry (FTICR MS) is confined in the radial direction by a strong homogeneous magnetic field, and in the axial direction by a three-dimensional quadrupolar electrostatic trapping well. The interaction of the ions with these fields results in three modes of motion with characteristic frequencies: cyclotron, axial, and magnetron. The cyclotron frequency, which is in a plane perpendicular to the magnetic field, is the most dependent on the m/z of the ion, and is, therefore, the most analytically useful of the three. Axial motion is parallel to the magnetic field and results from a centrally directed restoring force created by the trapping plate electrodes. As a result of the finite dimensions of the trapping field electrodes, there exists a radial component to the trapping electric field. The interaction of the ion with the radial component of the electric and the magnetic fields causes a slow precession of an ion cloud's guiding center. Ions undergoing this precession, known as the magnetron mode, have decreased cyclotron frequencies.

A small decrease in the cyclotron frequency is not of concern given that the conversion of frequency to mass can be calibrated. A problem arises, however, when the extent of this decrease is different for ions that have different mode amplitudes (i.e., cyclotron, axial, and

Address reprint requests to: Michael L. Gross, Department of Chemistry, Washington University, Campus Box 1134, One Brookings Drive, St. Louis, MO, 63130, mgross@wustl.edu.

**Publisher's Disclaimer:** This is a PDF file of an unedited manuscript that has been accepted for publication. As a service to our customers we are providing this early version of the manuscript. The manuscript will undergo copyediting, typesetting, and review of the resulting proof before it is published in its final citable form. Please note that during the production process errors may be discovered which could affect the content, and all legal disclaimers that apply to the journal pertain.

<sup>© 2010</sup> Elsevier B.V. All rights reserved.

magnetron). The electrical potential inside of the trap is only approximately quadrupolar, and therefore, the magnitude of the outwardly directed radial electric field varies non-linearly with mode amplitudes (i.e., ion position in the trap). As a result, the cyclotron frequency depends on not only its m/z value but also its mode amplitudes within the trap. This variation in cyclotron frequency ultimately reduces performance by decreasing resolving power, signal-to-noise ratio, and mass accuracy.

New electrically compensated trap designs hold significant promise to improve the performance of FTICR MS [1-24] by reducing the deleterious effects of the nonlinearities in the electrical field. We reviewed in detail most of the research on trap compensation in a book chapter [25], and we won't repeat this perspective here. In this paper, we will examine more deeply the consequences of trap compensation using a strategy we recently reported [23] on the behavior of ions. In the research, we explored the increase in transient lifetimes, which are accompanied by an increase in mass resolving power and signal-to-noise (S/N) ratio, as well as investigated the relationship between ion number and observed cyclotron frequency differences observed in an uncompensated and a compensated FTICR trap.

## 2. Methods

The test compounds used, with the exception of the protein hTRF2, were obtained from Sigma Aldrich (St. Louis, MO). The human telomeric repeat binding factor 2 (hTRF2) was obtained from S. Akashi at Yokohama City Univ., Japan, who expressed it in E. coli. These test compounds were mixed at various ratios with 2,5-dihydroxybenzoic acid used as a MALDI matrix. After mixing, the solutions of matrix and test compound were spotted on a 196-well stainless steel MALDI plate and allowed to dry. The plate was then introduced into the mass spectrometer, where the test compounds were ionized and detected.

The mass spectrometer was a 7-T IonSpec (now Varian) ProMALDI FTMS (Lake Forest, CA) outfitted with a custom electrically compensated cylindrical ICR trap, as described elsewhere [23]. Briefly, the compensated trap has the same overall dimensions as the original unmodified trap, but was constructed with three pairs of auxiliary ring electrodes to which the compensation voltages were applied. The excite/detect region of the compensated trap was smaller than that of the unmodified trap in order to accommodate the auxiliary ring electrodes without increasing the overall size of the trap.

Mass spectra were acquired in the compensated mode by applying independent non-zero voltages, determined by tuning [26], to each of the auxiliary rings. Those in the uncompensated mode were acquired by applying the same zero potential to each of the auxiliary rings. The trapping plates and inner rings, which supply the axial trapping well, were held at 1 V during detection in the compensated mode, while they were set at 0 and 1 V, respectively, for the uncompensated mode. Acquiring the spectra in this way allowed us to easily make comparisons between the compensated and uncompensated modes without having to replace an unmodified trap with a modified one, a process which requires vacuum cycling and considerable time.

All other operating parameters including excitation amplitude and duration, ion cooling conditions, and trapping were the same for experiments in which the compensated was compared with the uncompensated trap. The experimental details are available in [23] and [26].

Once the transient data were acquired, they were exported to a Fortran program for calculation of the magnitude mode frequency centroid, mass resolving power (full width half height), and complex area of each spectrum. The complex area was chosen to integrate the peaks because it is a better measure of the initial amplitude of the time-domain signal

envelope than is the amplitude of the magnitude mode peak observed in the spectrum [27]. In our opinion, the complex area gives a better measure of the amount of charge (ions) that is in the trap than did the peak area functions of the commercial data system.

## 3. Results

## 3.1. Transient Lifetimes and mass resolving power in a compensated trap

After excitation in an FT ICR mass spectrometer, ions undergo coherent cyclotron motion until the ions are dephased and signal is lost. Ultra high vacuum of the detection region assures that the mean free path of the ion is long, reducing the probability of dephasing by ion-neutral collisions. Other causes for dephasing are the slight differences in the cyclotron frequencies of ions having the same m/z [1,28].

Properly implemented, electrical trap compensation has the ability to reduce the variation in frequency as a function of mode amplitudes, thereby decreasing dephasing. In the experiments reported here, the background pressure in the uncompensated mode is the same as that of the compensated mode; thus, any increase in observed transient lifetime depends only on the ability of trap compensation to reduce the dephasing caused by variation in the cyclotron frequency as a function of various ion mode amplitudes (see Figure 1(a) for a comparison of transients acquired for [Arg]<sup>8</sup>-vasopressin in the compensated and uncompensated mode).

As a consequence of a longer lived transient, the compensated mode provides narrower peak widths and increased mass resolving power. The relationship between resolving power and transient lifetime is given by equation 1, where *f* is the cyclotron frequency and *t* is the observation time. The factor in the denominator depends on whether spectral apodization is employed and on the apodization function that is used. When no apodization is utilized, 1.206 is used in the denominator. For the two commonly employed apodization functions, Blackman and Hann apodizations, the denominators in the equations are 2.6 and 2, respectively [29]. Equation 1 reveals increased mass resolving power can be achieved by increasing the magnetic field strength and/or by extending the transient observation time.

$$RP_{fwhh} = \frac{f * t}{1.206} \tag{1}$$

There is always a tradeoff between observed S/N and mass resolving power. For FTICR MS, increasing the transient observation time increases the mass resolving power. Ultimately, however, longer transients can decrease signal intensity owing to a loss of phase coherence in the ion cloud or a reduction in cyclotron orbit size. Loss of phase coherence is caused by slight variations in cyclotron frequency for ions of the same *m/z* undergoing the same number of ion neutral collisions. Electrical trap compensation reduces the variation in frequency spread caused by nonlinearities in the trapping electric field but does not completely eliminate it. Variations in frequency can also be caused by an inhomogeneity in the magnetic field, but this has not yet been addressed for compensated traps operated over a wide mass range. Given that an ion of *m/z* 1000 in a 7-T magnetic field makes 100,000 revolutions per sec about the center of the trap, even part-per-million variations in the cyclotron frequency of the ion cloud will lead to dephasing.

The second source of ion cloud dephasing is ion neutral collisions, which are reduced by operating instruments under ultra high vacuum. Although the background pressure in most modern FTICR instruments is approximately  $10^{-10}$  torr, ion-neutral collisions still occur, especially with long acquisition times. At a pressure of  $10^{-10}$  torr, the frequency of ion-

neutral collision is estimated to be 0.003 Hz (~ 1 collision every 333 s). Given that ion-neutral collisions do not contribute significantly to the loss of signal intensity with time, the greater contributor to ion-cloud dephasing is the slight variations in cyclotron frequency.

Signal intensity can also diminish owing to a loss of energy from the cyclotron motion of the ions. This loss arises because the ions are doing work on the electrons in the detection circuit; consequently, energy is removed from the cyclotron mode, and its radius shrinks, causing a decrease in the observed signal intensity [28]. This is not a major effect and, under certain circumstances, decreases as m/z increases.

Irrespective of the mechanism by which the signal intensity decreases, the optimum observation time that strikes a balance between the observed peak intensity and mass resolving power is approximately three times the decay constant of the transient envelope,  $\tau$  [30]. At this time, the mass resolving power has increased to ~95% of its maximal value, whereas the signal still retains 30% of its initial amplitude. By fitting the transient envelopes in Figure 1(b) with an exponential decay function, we determined that  $\tau$  for the compensated mode was >200 s, whereas for the uncompensated mode  $\tau$  was ~20 s. Trap compensation affords an order of magnitude increase in transient lifetime in this example. Based on the rule that the optimum observation time is  $3\tau$ , the observation time for the transient acquired in the compensated mode could have been >600 s. Transient acquisition for this time, however, is not only impractically long but also demanding of computational requirements. Nevertheless, we achieved a significant increase in transient lifetime by using trap compensation owing to a decrease in the nonlinearity of the trapping electric field; this decrease results in a lower sensitivity to frequency variation as a function of ion mode amplitudes (i.e., ion position).

As variations in ion cyclotron frequency are reduced, the number of ions required to form a coherent packet also decreases [31,32]. Phase locking of an ion cloud that contains ions of the same m/z results in artificially lower peak widths. In the limit, where all ions of the same m/z have the same frequency regardless of mode amplitude, one cannot distinguish between an ion cloud that is phase-locked and one that is not. Along with an increase in mass resolving power comes an increase in S/N obtained by decreasing the spread in frequencies of a single m/z at a constant observation time. Given that peak area is a measure of ion number, the same ion count at improved mass resolving power gives an increase in S/N [33].

#### 3.2. Mass resolving power as a function of m/z

We employed test compounds giving  $[M + H]^+$  ions of different m/z values, ranging from  $[Arg]^8$ -vasopressin (m/z 1084) to cytochrome C ( $m/z \sim 12,500$ ), to compare the mass resolving powers obtained in the compensated mode to those achievable in the uncompensated mode. A log/log plot of observed mass resolving power (FWHH) versus m/z (transient observation time of 210 s) (Figure 2) shows that the compensated mode offers a significant increase in mass resolving power (by at least a factor of three) over that achieved in the uncompensated mode for the mass range studied. For  $[Arg]^8$ -vasopressin (m/z 1084), the m/z where the compensation voltages were tuned, the compensated mode achieved on average an order of magnitude increase in mass resolving power compared to that obtained in the uncompensated mode. The mass resolving powers obtained in the compensated mode do not always reach the theoretical maximum for the observation times employed. One reason is that compensation voltages, which were tuned at a single m/z, are not optimum for ions of other m/z values. Variations in the magnetic field also affect the cyclotron frequency, and these effects are mass dependent.

As the m/z of an ion increases, the full width at half height (mass resolving power) decreases, if all other factors remain the same, because the frequency decreases with m/z

(equation 1). Cytochrome C ( $m/z \sim 12,500$ ) appears to be an outlier to the trend observed in the compensated mode (Fig. 2), but the lower resolving power is due to the shorter transient acquisition time used for the cytochrome C transient (105 s) versus that used for the other compounds of lower m/z (210 s). For these evaluations, we looked at those components of an isotope cluster that are separated by one m/z but not those that exist at a single m/z (the high resolution isotopomers) [23]. An analogous deviation was not observed in the uncompensated mode because the transient signal had decayed before the data acquisition was complete and, therefore, was not time limited. As discussed earlier for the data in Figure 1, the transient lifetime of an ion cloud in the uncompensated mode is an order of magnitude lower ( $\sim 20$  s) than that in the compensated mode (> 200 s). Using these values as estimates of transient lifetimes at m/z values higher than 1084, we conclude that the transient observation time was greater than  $3\tau$  in the uncompensated mode but approximately equal to  $\tau$  in the compensated mode acquisitions.

## 3.3. Improved signal-to-noise ratio in compensated mode

We used insulin oxidized b-chain and TRF2 to assess the improvement in signal-to-noise ratio (S/N) afforded by trap compensation. To accomplish this, we acquired several spectra while switching between the compensated and uncompensated modes. The different modes were interdigitated in this way to reduce the influence of shot-to-shot variability commonly found in MALDI. Compensation results in an increase of at least an order of magnitude in S/N when compared to that achieved in the uncompensated trap under these experimental conditions (Fig. 3). Of the mass spectra from the uncompensated trap for the insulin oxidized b-chain, only one had signal that was greater than three times the noise level. In the mass spectra of the protein hTRF2, no signal was detected above the noise. Increasing the laser power to desorb the sample did not produce signal in the uncompensated mode. When the laser power is sufficiently high that it completely ablates the spotted material over the irradiated area, no additional signal can be gained by further increasing the laser power. By using a fixed laser power, which on average produced a constant number of ions, the experiments demonstrate that the compensated mode affords a better detection limit than does the uncompensated mode.

## 3.4. Frequency as a Function of Ion Number

Generally as ion number increases, the observed cyclotron frequency of the ion of interest decreases linearly [34]. Given this phenomenon, we were initially surprised that the observed cyclotron frequency of [Arg]<sup>8</sup>-vasopressin (*m*/*z* 1084) initially increased with increasing complex area (see Figure 4(a)) in the uncompensated mode, particularly when we had chosen an orbit radius that is ~ 40% the trap width. Leach et al. [35] observed the same increase in frequency with increasing ion number both experimentally and in particle-in-cell calculations when using a non-ideal quadrupolar trapping potential. This initial increase would have a significant impact on mass measurement accuracy because the calibration equations used in FTICR assume a decreasing linear relationship between ion frequency and ion number or density. Accounting for this relationship is necessary for high mass measurement accuracy as it is difficult to fill the trap with exactly the same number of ions for each experiment. Automatic Gain Control<sup>TM</sup> [36] on the Thermo Fisher LTQ-FT is one approach to combat variation in ion number between experiments. This hybrid mass spectrometer uses a Paul trap to control precisely the number of ions that are injected into the ICR trap for each experiment, minimizing variations in ion number.

To understand why the frequency initially increases as a function of ion number (as measured by complex area) in the uncompensated mode, the acquired transient was segmented prior to FFT to see how the peaks evolved with time. The window used for segmenting was ½ of the width of the transient (~50 s), and the position of the window's

leading edge was varied, so that it would sample different portions of the transient with each analysis. The results of the segmented transient analysis (Figure 5) revealed that the increase in frequency with increasing ion number (observed in the uncompensated mode) is due a split peak. The two portions of the split peak interact in such a way that the high mass resolving power, low-frequency portion of the peak, is increased in frequency, whereas the opposite applies for the low mass resolving power, high-frequency portion. This phase locking of the ion cloud causes an increase in frequency because we typically only observe the frequency centroid of the low-frequency peak seen at high mass resolving power in the mass spectrum. These trends in frequency shift can be seen in (b) and (c) of Figure 5. As ion number increases, the likelihood and rate of phase locking also increase [31]. Ultimately, the ion number in the uncompensated mode became sufficiently high that one cannot observe the split peak because the ion cloud is phase-locked prior to the start of the detection event. Any further increase in ion number beyond this point results in a decrease in the observed cyclotron frequency, as expected (see Figure 4(a)).

We showed earlier that electrical trap compensation reduces the variation in frequency as a function of mode amplitude caused by nonlinearities in the trapping electric field. Because electrical trap compensation eliminates peak splitting over the range of cyclotron radii where the trap is compensated, the relationship between frequency and ion number in the compensated mode should be more ideal. In fact, the ion frequency decreases in a more linear fashion with increasing ion number in the compensated mode than in the uncompensated mode (see Figure 4(b) for the frequency of [Arg]<sup>8</sup>-vasopressin (m/z 1084) as a function of complex area (ion number) in the compensated mode). This being the case, it is reasonable to assume that improved mass measurement accuracy should accrue to measurements in a compensated trap because it conforms more closely to the theory that underlies the mass calibration equations.

## 4. Conclusions

Trap compensation improves mass resolving power and S/N of FTICR MS [23] owing to increases in the linearity of the trapping electric field and the resultant ion-cloud coherence and transient lifetimes. In fact, transient lifetimes in the compensated mode increase by approximately an order of magnitude when compared to those in the uncompensated mode. As a result, the mass resolving power increased over a m/z range of 1084 ([Arg]8-vasopressin) to ~12,500 (cytochrome C), a realistic range for most biological mass spectrometric applications, especially when using electrospray ionization. For spectral peaks containing the same number of ions, S/N increased with increasing mass resolving power, as was first described in 1980 [33]. The increase in S/N afforded by trap compensation is approximately an order of magnitude.

Reducing the nonlinearities of the trapping electric potential can eliminate peak splitting. As a consequence, the relationship between observed cyclotron frequency and ion number is more linear, and this improved linearity should lead to more control in mass calibration and increased mass measurement accuracy.

## **Acknowledgments**

This work was supported by the NIH National Center for Research Resources, Grant No. 2P41RR000954.

#### References

[1]. Guan S, Marshall AG. Ion traps for Fourier transform ion cyclotron resonance mass spectrometry: principles and design of geometric and electric configurations. International Journal of Mass Spectrometry and Ion Processes. 1995; 146/147:261–296.

[2]. Naito Y, Fujiwara M, Inoue M. Improvement of the electric field in the cylindrical trapped-ion cell. International Journal of Mass Spectrometry and Ion Processes. 1992; 120:179–192.

- [3]. Vartanian VH, Hadjarab F, Laude DA. Open cell analog of the screened trapped-ion cell using compensation electrodes for Fourier transform ion cyclotron resonance mass spectrometry. International Journal of Mass Spectrometry and Ion Processes. 1995; 151:175–187.
- [4]. Kaiser NK, Bruce JE. Observation of Increased Ion Cyclotron Resonance Signal Duration through Electric Field Perturbations. Analytical Chemistry. 2005; 77:5973–5981. [PubMed: 16159130]
- [5]. Kaiser NK, Bruce JE. Reduction of ion magnetron motion and space charge using radial electric field modulation. International Journal of Mass Spectrometry. 2007; 265:271–280.
- [6]. Hunter RL, Sherman MG, McIver RT Jr. An elongated trapped-ion cell for ion cyclotron resonance mass spectrometry with a superconducting magnet. International Journal of Mass Spectrometry and Ion Physics. 1983; 50:259–274.
- [7]. Van Dyck RS Jr. Schwinberg PB. Preliminary proton/electron mass ratio using a compensated quadring Penning trap. Physical Review Letters. 1981; 47:395–398.
- [8]. Van Dyck RS Jr. Wineland DJ, Ekstrom PA, Dehmelt HG. High mass resolution with a new variable anharmonicity Penning trap. Applied Physics Letters. 1976; 28:446–448.
- [9]. Rempel DL, Ledford EB Jr. Huang SK, Gross ML. Parametric mode operation of a hyperbolic Penning trap for Fourier transform mass spectrometry. Analytical Chemistry. 1987; 59:2527–2532. [PubMed: 3688441]
- [10]. Gabrielse G, MacKintosh FC. Cylindrical Penning traps with orthogonalized anharmonicity compensation. International Journal of Mass Spectrometry and Ion Processes. 1984; 57:1–17.
- [11]. Wang M, Marshall AG. A "screened" electrostatic ion trap for enhanced mass resolution, mass accuracy, reproducibility, and upper mass limit in Fourier-transform ion cyclotron resonance mass spectrometry. Analytical Chemistry. 1989; 61:1288–1293. [PubMed: 2757208]
- [12]. Hanson CD, Castro ME, Kerley EL, Russell DH. Field-corrected ion cell for ion cyclotron resonance. Analytical Chemistry. 1990; 62:520–526.
- [13]. Vartanian VH, Laude DA. Optimization of a fixed-volume open geometry trapped ion cell for Fourier transform ion cyclotron mass spectrometry. International Journal of Mass Spectrometry and Ion Processes. 1995; 141:189–200.
- [14]. Knobeler M, Wanczek KP. Theoretical investigation of improved ion trapping in matrix-assisted laser desorption/ionization Fourier transform ion cyclotron resonance mass spectrometry: independence of ion initial velocity. International Journal of Mass Spectrometry and Ion Processes. 1997; 163:47–68.
- [15]. Jackson GS, White FM, Guan S, Marshall AG. Matrix-shimmed ion cyclotron resonance ion trap simultaneously optimized for excitation, detection, quadrupolar axialization, and trapping. Journal of the American Society for Mass Spectrometry. 1999; 10:759–769.
- [16]. Bruce JE, Anderson GA, Lin C-Y, Gorshkov M, Rockwood AL, Smith RD. A novel high-performance Fourier transform ion cyclotron resonance cell for improved biopolymer characterization. Journal of Mass Spectrometry. 2000; 35:85–94. [PubMed: 10633238]
- [17]. Marshall AG. Milestones in Fourier transform ion cyclotron resonance mass spectrometry technique development. International Journal of Mass Spectrometry. 2000; 200:331–356.
- [18]. Barlow SE, Tinkle MD. "Linearizing" an ion cyclotron resonance cell. Review of Scientific Instruments. 2002; 73:4185–4200.
- [19]. Gooden JK, Rempel DL, Gross ML. Evaluation of different combinations of gated trapping, RF-only mode and trap compensation for in-field MALDI Fourier transform mass spectrometry. Journal of the American Society for Mass Spectrometry. 2004; 15:1109–1115. [PubMed: 15234369]
- [20]. Kim S, Choi MC, Kim S, Hur M, Kim HS, Yoo JS, Blakney GT, Hendrickson CL, Marshall AG. Modification of Trapping Potential by Inverted Sidekick Electrode Voltage during Detection To Extend Time-Domain Signal Duration for Significantly Enhanced Fourier Transform Ion Cyclotron Resonance Mass Resolution. Analytical Chemistry (Washington, DC, United States). 2007; 79:3575–3580.

[21]. Kaiser NK, Weisbrod CR, Webb BN, Bruce JE. Reduction of Axial Kinetic Energy Induced Perturbations on Observed Cyclotron Frequency. Journal of the American Society for Mass Spectrometry. 2008; 19:467–478. [PubMed: 18262433]

- [22]. Tolmachev AV, Robinson EW, Wu S, Kang H, Lourette NM, Pasa-Tolic L, Smith RD. Trapped-Ion Cell with Improved DC Potential Harmonicity for FTICR MS. Journal of the American Society for Mass Spectrometry. 2008; 19:586–597. [PubMed: 18296061]
- [23]. Brustkern AM, Rempel DL, Gross ML. An Electrically Compensated Trap Designed to Eighth Order for FTICR Mass Spectrometry. Journal of the American Society for Mass Spectrometry. 2008; 19:1281–1285. [PubMed: 18599306]
- [24]. Kaiser NK, Skulason GE, Weisbrod CR, Bruce JE. A Novel Fourier Transform Ion Cyclotron Resonance Mass Spectrometer with Improved Ion Trapping and Detection Capabilities. Journal of the American Society for Mass Spectrometry. 2009; 20:755–762. [PubMed: 19200753]
- [25]. Brustkern, AM.; Rempel, DL.; Gross, ML. Practical Aspects of Trapped Ion Mass Sectrometry. Radio Frequency-Only-Mode Event and Trap Compensation in Penning Fourier Transform Mass Spectrometry. In Press
- [26]. Brustkern AM, Rempel DL, Gross ML. A Tuning Method for Electrically Compensated Ion Cyclotron Resonance Mass Spectrometer Traps. Journal of the American Society for Mass Spectrometry. 2010; 21:451–454. [PubMed: 20060743]
- [27]. Huang, SKR.; Gross, ML. Problems With Quantification of Ion Abundances and a Proposed Solution; presented at the 32nd Annual Conference on Mass Spectrometry and Allied Topics; San Antonio, TX. May 27 June 1, 1984; D. L.
- [28]. Marshall AG, Hendrickson CL, Jackson GS. Fourier transform ion cyclotron resonance mass spectrometry: A primer. Mass Spectrometry Reviews. 1998; 17:1–35. [PubMed: 9768511]
- [29]. McIver, JRM.; Robert, T, Jr.. Fourier Transform Mass Spectrometry: Principles and Applications. IonSpec Corporation; Lake Forest: 2006.
- [30]. Marshall AG, Comisarow MB, Parisod G. Relaxation and spectral line shape in Fourier transform ion resonance spectroscopy. Journal of Chemical Physics. 1979; 71:4434–4444.
- [31]. Mitchell DW. Realistic simulation of the ion cyclotron resonance mass spectrometer using a distributed three-dimensional particle-in-cell code. Journal of the American Society for Mass Spectrometry. 1999; 10:136–152.
- [32]. Nikolaev EN, Heeren RMA, Popov AM, Pozdneev AV, Chingin KS. Realistic modeling of ion cloud motion in a fourier transform ion cyclotron resonance cell by use of a particle-in-cell approach. Rapid Communications in Mass Spectrometry. 2007; 21:3527–3546. [PubMed: 17944004]
- [33]. White RL, Ledford EB Jr. Ghaderi S, Wilkins CL, Gross ML. Resolution and Signal-to-Noise in Fourier Transform Mass Spectrometry. Analytical Chemistry. 1980; 52:1525–1527.
- [34]. Jeffries JB, Barlow SE, Dunn GH. Theory of space-charge shift of ion cyclotron resonance frequencies. Int. J. Mass Spectrom. Ion Processes. 1983; 54:169–187.
- [35]. Leach FE, Kharchenko A, Heeren RMA, Nikolaev E, Amster IJ. Comparison of Particle-In-Cell Simulations with Experimentally Observed Frequency Shifts Between Ions of the Same Mass-to-Charge in Fourier Transform Ion Cyclotron Resonance Mass Spectrometry. Journal of the American Society for Mass Spectrometry. 2010; 21:203–208. [PubMed: 19896390]
- [36]. Syka JEP, Marto JA, Bai DL, Horning S, Senko MW, Schwartz JC, Ueberheide B, Garcia B, Busby S, Muratore T, Shabanowitz J, Hunt DF. Novel Linear Quadrupole Ion Trap/FT Mass Spectrometer: Performance Characterization and Use in the Comparative Analysis of Histone H3 Post-translational Modifications. Journal of Proteome Research. 2004; 3:621–626. [PubMed: 15253445]

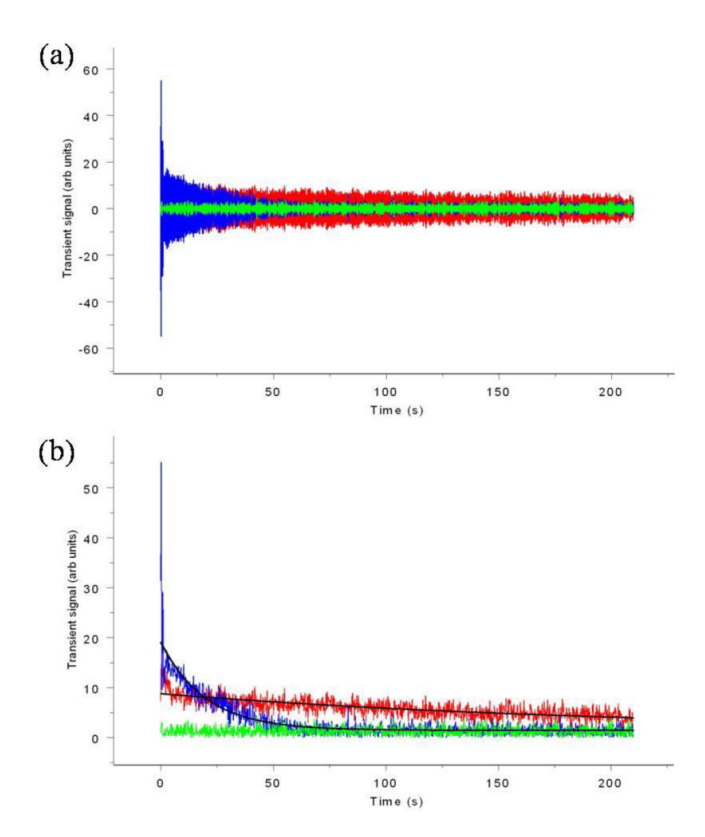


**Figure 1.**(a) Transients for [Arg]<sup>8</sup>-vasopressin acquired in the compensated (red) and uncompensated modes (blue). The green trace indicates the noise level. The transients are the inverse Fourier transform of the mass range of interest. (b) The transient envelope for the compensated (red) and uncompensated mode (blue). The decay constant for the compensated mode was ~200 s, whereas that of the uncompensated mode was ~20 s.

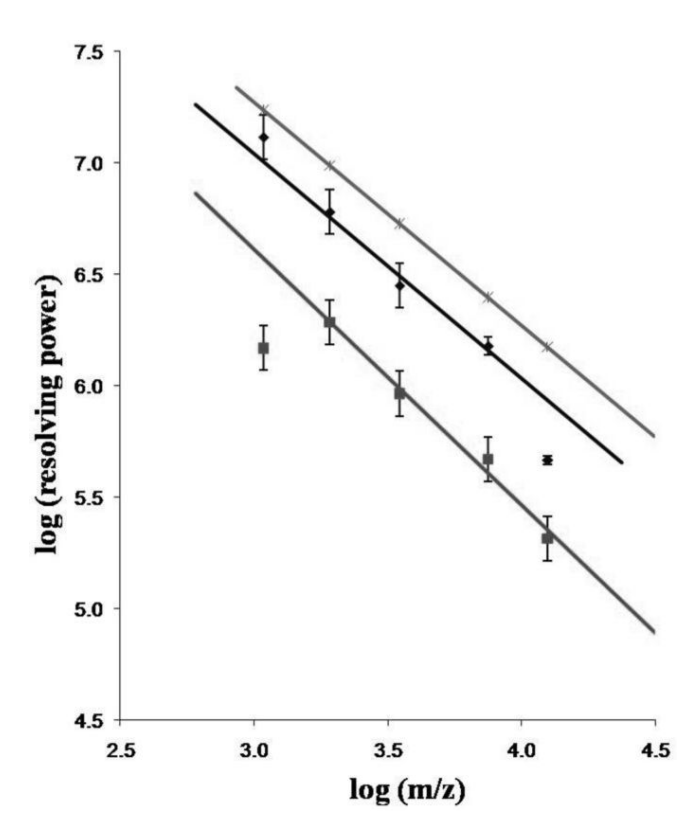


Figure 2. A log/log plot of mass resolving power versus m/z comparing the uncompensated mode (squares) to the compensated mode (diamonds). The m/z values range from 1084 ([Arg]<sup>8</sup>-vasopressing) to ~12,500 (cytochrome C). Included for reference is a plot of the theoretical resolving powers calculated for an observation time of 210 s (x's). As noted in the text, the transient observation time for cytochrome C (log m/z = 4.1) was lower (105 s) than that used for the other ions (210 s), which accounts for the deviation from the straight-line plot.

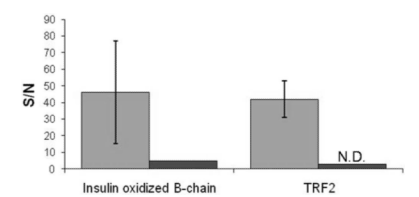


Figure 3. Comparison of the S/N obtained in the compensated (light grey) and uncompensated (dark grey) modes for insulin oxidized b-chain and TRF2. The large error bars for the compensated mode result from the variability that commonly occurs in MALDI. Only one of the spectra obtained in the uncompensated mode for insulin oxidized b-chain had a S/N > 3. In the case of TRF2, none of the spectra obtained in the uncompensated mode had a S/N > 3, so the result was consider not detected (N.D.) and the average value was set to 3 in the bar graph.

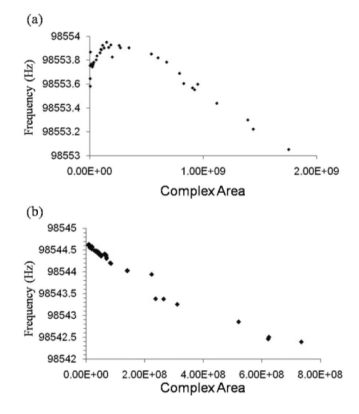
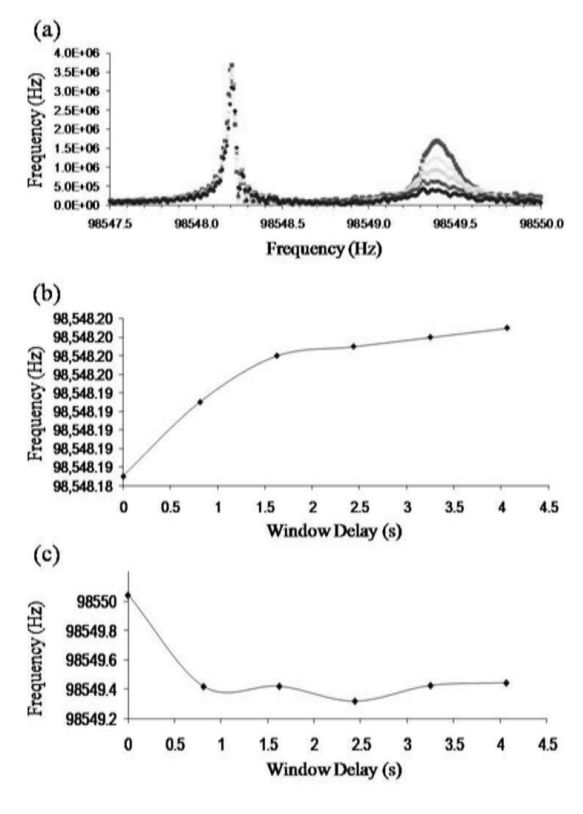


Figure 4. The observed cyclotron frequency of  $[Arg]^8$ -vasopressin as a function of complex area (ion number) in the (a) uncompensated mode and (b) compensated mode.



**Figure 5.**(a) Segmented transient analysis of [Arg]<sup>8</sup>-vasopressin obtained by utilizing a window that was ¼ the total acquisition duration and varying the position (in terms of time) of its leading edge. The measured frequency centroids of the high resolving power peak (b) and the low resolving power peak (c) as a function of the location of the analysis window.